Published in final edited form as:
Biochim Biophys Acta. 2018 April ; 1863(4): 467–478. doi:10.1016/j.bbalip.2018.01.011.

Lysosomal acid lipase regulates fatty acid channeling in brown adipose tissue to maintain thermogenesis

Madalina Duta-Mare[1], **Vinay Sachdev**[1], **Christina Leopold**[1], **Dagmar Kolb**[1,2], **Nemanja Vujic**[1], **Melanie Korbelius**[1], **Dina C. Hofer**[3], **Wenmin Xia**[3], **Katharina Huber**[3], **Martina Auer**[1], **Benjamin Gottschalk**[1], **Christoph Magnes**[4], **Wolfgang F. Graier**[1,5], **Andreas Prokesch**[1], **Branislav Radovic**[1,5], **Juliane G. Bogner-Strauss**[3,5], and **Dagmar Kratky**[*,1,5]

[1]Gottfried Schatz Research Center, Medical University of Graz, Graz, Austria

[2]Center for Medical Research, Medical University of Graz, Graz, Austria

[3]Institute of Biochemistry, Graz University of Technology, Graz, Austria

[4]Health, Bioanalytik und Metabolomics, Joanneum Research, Graz, Austria

[5]BioTechMed-Graz, Graz, Austria

Abstract

Lysosomal acid lipase (LAL) is the only known enzyme, which hydrolyzes cholesteryl esters and triacylglycerols in lysosomes of multiple cells and tissues. Here, we explored the role of LAL in brown adipose tissue (BAT). LAL-deficient (Lal-/-) mice exhibit markedly reduced UCP1 expression in BAT, modified BAT morphology with accumulation of lysosomes, and mitochondrial dysfunction, consequently leading to regular hypothermic events in mice kept at room temperature. Cold exposure resulted in reduced lipid uptake into BAT, thereby aggravating dyslipidemia and causing life threatening hypothermia in Lal-/- mice. Linking LAL as a potential regulator of lipoprotein lipase activity, we found Angptl4 mRNA expression upregulated in BAT. Our data demonstrate that LAL is critical for shuttling fatty acids derived from circulating lipoproteins to BAT during cold exposure. We conclude that inhibited lysosomal lipid hydrolysis in BAT leads to impaired thermogenesis in Lal-/- mice.

Keywords

Brown adipose tissue; LAL deficiency; Lysosome; UCP1; Thermogenesis; Dyslipidemia

[*]Corresponding author: Dagmar Kratky, Gottfried Schatz Research Center, Medical University of Graz, Graz, Austria, Neue Stiftingtalstrasse 6/6, 8010 Graz, Austria; phone +43-316-385-71965, fax: +43-316-385-79615, dagmar.kratky@medunigraz.at.

Author contributions

MDM and DKr conceived and designed the study and wrote the paper. MDM, VS, CL, DKo, NV, MK, DH, WX, KH, CM, MA, BG, and BR contributed to data collection and analyses. JBS, AP, and WFG contributed to study design and data interpretation. All authors critically revised the manuscript and have read and approved the final version. DKr is responsible for the integrity of the work as a whole.

Europe PMC Funders Author Manuscripts

1 Introduction

Lysosomal acid lipase (LAL) hydrolyzes cholesteryl esters (CE), triacylglycerols (TG), and retinyl esters within lysosomes after lipoprotein uptake or through autophagy, respectively [1–3]. In humans and mice, absence or dysfunction of LAL results in excessive lysosomal lipid accumulation, supporting the notion that LAL is responsible for lipid degradation at acidic pH in lysosomes [4–7]. In general, the disease severity in humans (collectively referred to as LAL deficiency, LAL-D) is primarily based on the absence or amount of residual LAL activity determined by LAL gene mutations. Whereas patients with total loss in LAL activity hardly survive one year of age, residual enzymatic activity is found in individuals with cholesteryl ester storage disease, a rare but still underdiagnosed condition. These patients survive beyond mid-age but develop hepatic and atherosclerotic complications, leading eventually to premature mortality [8, 9]. Beside severe hepatomegaly, the phenotype of Lal-deficient (-/-) mice includes progressive loss of white adipose tissue (WAT) and brown adipose tissue (BAT) during aging [5]. Our previous study revealed reduced circulating leptin concentrations in the fed state, hypercholesterolemia, and hypoglycemia but improved glucose tolerance and insulin sensitivity in Lal-/- mice [10].

In mammals, BAT is responsible for non-shivering thermogenesis and thereby plays an important role in maintaining body temperature homeostasis, particularly in a cold environment. BAT is morphologically and functionally different from WAT due to its multilocular lipid droplets (LD), high abundance of mitochondria, increased metabolic rate, and the presence of uncoupling protein 1 (UCP1) [11, 12]. UCP1 has a unique role to uncouple mitochondrial respiration from ATP production and thereby supports thermogenesis during cold exposure [13]. Additionally, the uncoupling activity of UCP1 is increased by fatty acids (FA) independently of their metabolism [14]. Cold stimulates BAT via β3 adrenergic receptor signaling, which triggers the utilization of FA and glucose as substrates for thermogenesis. To fuel this process, TG stored in cytosolic LD of brown adipocytes are initially catabolized via lipolysis mediated by the consecutive action of adipose triglyceride lipase (ATGL), hormone-sensitive lipase (HSL), and monoglyceride lipase [15, 16]. As brown adipocytes have limited fat storage capacity, LD are continuously replenished by the supply of FA from the blood stream [15]. For this purpose, food intake is increased during cold and TG (in form of circulating chylomicrons) deliver sufficient FA to activated BAT [11]. In addition, WAT serves as TG depot to release FA in times of need, like during nutrient restriction or high metabolic demand via ATGL-mediated hydrolysis [17].

Beside cholesterol, excessive TG-rich lipoprotein (TRL) concentrations in the blood cause dyslipidemia, a risk factor for atherosclerosis and the metabolic syndrome [18, 19]. New hope for hyperlipidemia treatment arose when TRL were shown to be massively cleared by activated BAT [20]. Intensive research in the last decade has revealed multiple benefits of BAT activation in reducing not only plasma TG but also cholesterol concentrations, improving glucose tolerance and insulin sensitivity, and decreasing fat depots [21, 22]. Enhancing BAT activity was reported to protect from atherosclerosis development by accelerating blood cholesterol clearance in mice expressing functional apolipoprotein E and low-density lipoprotein receptor [22]. Besides lipoprotein lipase (LPL)-mediated lipolysis of TRL, an alternative uptake of entire lipoprotein particles by BAT was suggested. This

process is dependent on LPL/CD36 tandem action and is possibly mediated by increased endothelial permeability or transcytosis [20]. To which extent holoparticle uptake by BAT affects thermogenesis is still unclear [23]. This type of substrate processing would require receptor-mediated endocytosis and consequently lysosomal lipolytic degradation via LAL [1].

Due to major metabolic adaptations caused by LAL deficiency and reduced body adiposity, we aimed to study the consequences of LAL deficiency on BAT function and thermogenesis. Here we show that Lal-/- mice have preserved weight but modified morphology and defective functionality of BAT. LAL deficiency strongly decreases UCP1 protein expression leading to transient hypothermia in mice housed at room temperature (RT). When kept at 5°C, Lal-/- mice present life threatening cold intolerance. The current study provides evidence that LAL deficiency causes accumulation of lipid-laden lysosomes in BAT and that FA released by acid hydrolysis serve as thermogenic activators through multiple mechanisms. Importantly, cold exacerbates dyslipidemia in Lal-/- mice due to reduced FA uptake in BAT, suggesting that restoring blood lipoprotein balance depends on functional LAL.

2 Material and Methods

2.1 Animals

All experiments were performed using female and male Lal-/- mice and their corresponding wild type (WT) littermates [5] on a C57BL/6 background [10] aged 20 weeks unless stated otherwise. The mice were maintained in a clean environment and a regular light-dark cycle (12 h light, 12 h dark) with unlimited access to chow diet (4% fat and 9% protein; Altromin 1324, Lage, Germany) and water. For cold exposure experiments, Lal-/- and WT mice were kept at 5°C with food and water *ad libitum*. Core body temperature was measured using a rectal probe thermometer (Physitemp Instruments, Inc., Clifton, NJ). Blood glucose was determined using Accu-Chek® Active glucometer and glucose strips (Roche Diagnostics GmbH, Mannheim, Germany).

All animal experiments were performed in compliance with national laws and were approved by the Austrian Federal Ministry of Science, Research, and Economy, Vienna, Austria, in accordance with the European Directive 2010/63/EU.

2.2 Plasma lipid and creatine phosphokinase activity measurements

Blood was collected by facial vein puncture and plasma was prepared within 20 min. TG, total cholesterol (TC), and free cholesterol (FC) concentrations were determined in plasma from mice using enzymatic kits (DiaSys, Holzheim, Germany). Plasma free glycerol (FG) and free fatty acid (FFA) concentrations were determined using Free Glycerol Reagent (Sigma-Aldrich, St. Louis, MO) and NEFA-HR kit (Wako Life Sciences, Mountain View, CA), respectively. Lipoprotein fractions were separated from 200 μl pooled plasma from each group using fast protein liquid chromatography as previously described [24]. Creatine phosphokinase activity in plasma samples was measured using a Spotchem EZ analyzer and test strips (A. Menarini GmbH, Vienna, Austria).

2.3 Energy metabolism *in vivo*

Assessment of energy intake and energy expenditure was performed using a climate-controlled indirect calorimetry system (TSE PhenoMaster, TSE Systems, Bad Homburg, Germany). WT and Lal-/- mice were housed in automatic metabolic cages in a regular light-dark cycle (12 h light, 12 h dark) with free access to food and water. Weight-matched female mice were acclimatized for 48 h before experiments. During gradual cooling, the temperature was decreased from 22°C to 5°C over a period of 7 days. O_2 consumption, CO_2 production, and locomotor activity (using infrared sensor frames) were measured every 15 min. Carbohydrate and lipid oxidation rates were determined as described [25] and converted from mg/h into kcal/h.

2.4 Mitochondrial respiration measurement

WT and Lal-/- mice were housed at 5°C for 4 h. Oxygen consumption rate of freshly isolated BAT was determined using a Clark electrode (Strathkelvin Instruments, Glasgow, Scotland) as previously described [26] with minor modifications. Approximately 20 mg of BAT were minced and transferred into the MT200A measurement chamber containing 1 ml of 100% air-saturated respiration buffer (2% BSA, 100 mg/dl or 450 mg/dl D-glucose, 6 mg pyruvate). Maximal respiration was measured after the addition of 25 μM carbonyl cyanide-4-(trifluoromethoxy) phenylhydrazone (FCCP) to the respiration buffer. Oxygen consumption rates were normalized to tissue weight and calculated as μg O_2/min/tissue.

2.5 Determination of BAT and SM acyl-CoA and acyl-carnitine concentrations

Female mice were exposed to cold for 3 h and BAT was collected and snap-frozen in liquid nitrogen. Tissue samples were homogenized for 2 x 30 s using a tissue homogenizer (Precellys 24, Bertin Technologies, Montigny-le-Bretonneux, France). Concentrations of acyl-CoAs and carnitine esters (semi-quantitative) were measured by on-line solid phase extraction liquid chromatography-mass spectrometry as previously described [27].

2.6 Reverse transcription and quantitative real-time PCR

Two μg of total RNA were reverse transcribed (High Capacity cDNA Reverse Transcription Kit; Applied Biosystems, Carlsbad, CA). Quantitative real-time PCR of samples analyzed in duplicate was performed on a Roche LightCycler 480 (Roche Diagnostics, Palo Alto, CA) using the QuantiFastTM SYBR® Green PCR Kit (Qiagen, Valencia, CA). Expression profiles and associated statistical parameters were calculated using the $2^{-\Delta\Delta CT}$ method normalized to the expression of cyclophilin A as housekeeping gene. Primer sequences are listed in the supplement.

2.7 Western blotting analysis

BAT was lysed in RIPA buffer and protein concentrations were quantitated (DC™ Protein assay, Bio-Rad Laboratories, Hercules, CA). BAT lysates (40 μg protein) were separated by SDS-PAGE and transferred onto PVDF membranes. Non-specific binding sites of the membranes were blocked (5% solution of milk powder or 1% BSA in washing buffer) for 1 h. For detection of the proteins of interest, anti-rabbit polyclonal antibodies against UCP1 (Abcam, Cambridge, UK), LC3B, AKT, and anti-mouse polyclonal antibody against p-AKT

(all purchased from Cell Signaling Technology, Danvers, MA) were used at a dilution of 1:1,000. Polyclonal anti-rabbit calnexin (1:1,000) (Santa Cruz, Heidelberg, Germany) or GAPDH (1:1,000) (Cell Signaling Technology) were used as loading controls. HRP-conjugated goat anti-rabbit (1:2,500) and rabbit anti-mouse antibodies (1:500) (Dako, Glostrup, Denmark) were visualized by enhanced chemiluminescence detection on a ChemiDoc™ MP imaging system (Bio-Rad Laboratories).

2.8 Lipase activity assays

BAT from RT-housed female mice or from cold-exposed male mice was lysed in lysis buffer (100 mM potassium phosphate, 250 mM sucrose, 1 mM EDTA, 10 mM dithiothreitol (DTT), pH 7) and centrifuged at 10,000 x *g* and 4°C for 30 min. The protein content of the clear infranatant was determined by a Lowry assay (Bio-Rad). TG hydrolase activity was determined as recently described [28].

Immortalized brown adipogenic cells (iBACs) were lysed in lysis buffer (100 mM NaH_2PO_4, pH 6.8, 1 mM EDTA, 10 mM DTT, 0.5% NP-40, 0.02% sodium azid, protease inhibitors) and centrifuged for 10 min at 10,000 x *g*. LAL activity was estimated using the fluorogenic substrate 4-methyl-umbelliferyl-palmitate (4-MUP) as described [28].

2.9 [^{3}H]2-deoxy-D-glucose uptake

Female WT and Lal-/- mice aged 12 weeks were kept at 5°C with free access to food for 3 h. Thereafter, food was removed and the mice were intraperitoneally injected with glucose (1 g/kg body weight containing 2 μCi [^{3}H]2-deoxy-D-glucose in PBS). Mice were sacrificed 60 min post injection and radioactivity in tissue lysates was determined by liquid scintillation counting.

2.10 Fatty acid uptake

Female WT and Lal-/- mice aged 16 weeks were kept at 5°C with free access to food for 4 h. Thereafter, food was removed and the mice were gavaged with 100 μl corn oil containing 8 μCi [^{3}H]triolein. The mice were sacrificed 3 h post gavage and radioactivity in BAT lysates was determined by liquid scintillation counting.

2.11 Electron microscopy

We used male 6 and 20 week old mice in the fed state to assess BAT morphology at RT. For the electron micrographs from cold-exposed BAT, we used female 12 week old mice exposed to cold for 4 h with unlimited access to food and water with or without an additional corn oil gavage (100 μl). BAT was fixed in phosphate buffer/2.5% glutaraldehyde for 2 h, washed, post-fixed in phosphate buffer/OsO_4 for 2 h and 4x10 min in phosphate buffer. After dehydration, tissues were infiltrated (acetone and agar 100 epoxy resin, pure agar 100 epoxy resin) for 4 h, placed in agar 100 epoxy resin (8 h), transferred into embedding molds, and polymerized (48 h, 60°C). Sections stained with lead citrate and platine blue were imaged at 120 kV with a Tecnai G 2 FEI microscope (FEI, Eindhoven, Netherlands) equipped with a Gatan ultrascan 1000 CCD camera. LDs from 97 electron micrographs (each having a surface of 142.09 μm^2) per genotype were counted and analyzed by open source ImageJ software image processing and analysis in Java.

Europe PMC Funders Author Manuscripts

2.12 Toluidine blue staining

Female WT and Lal-/- mice aged 12 weeks were exposed to cold for 4 h in the fed state with or without an additional corn oil gavage (100 μl). BAT was collected and prepared as described in “Electron microscopy”. Thereafter, 2.5 μm-thick sections were stained with toluidine blue.

2.13 Immunofluorescence staining

Male WT and Lal-/- mice aged 20 weeks were exposed to cold for 2 h. Thereafter, BAT was dissected from interscapular regions, washed in PBS, fixed in 4% paraformaldehyde for 24 h, and transferred to PBS for storage. Tissue was embedded in paraffin, cut in 5 μm-thick sections, and mounted on Superfrost Plus slides (Menzel-Glaeser). Standard de-paraffinization was followed by boiling sections in 10 mM sodium citrate buffer (pH 6.0) for 7 min for antigen retrieval. Protein blocking was performed with UltraVision Protein Block (Thermo Fisher Scientific, Waltham, MA) and M.O.M.™-Blocking reagent (Vector Laboratories, Burlingam, CA). Slides were incubated with anti-cathepsin D (1:200, ab6313, Abcam) and anti-perilipin 1 antibodies (1:200, 9349, Cell Signaling Technology) for 30 min. Subsequently, slides were washed and incubated with a mixture of Alexa Fluor 488 goat anti-rabbit and Alexa Fluor 594 goat anti-mouse antibodies (both 1:500; Thermo Fisher Scientific) for 30 min at RT. Negative control for rabbit IgG (Dako) and negative control mouse IgG2a (Dako) generated non-specific staining. After staining, tissue sections were mounted with ProLong Gold antifade reagent (Thermo Fisher Scientific). Confocal images of samples were acquired with a Zeiss Observer Z.1 inverted microscope equipped with a Yokogawa CSU-X1 Nipkow spinning disk system, a piezoelectric z-axis motorized stage (CRWG3-200; Nippon Thompson Co., Ltd., Tokyo, Japan), and a CoolSNAP HQ2 CCD Camera (Photometrics, Tucson, AZ). Cells were excited with 488 nm and 568 nm laser lines (Visitron Systems, Puchheim, Germany) with exposure times of 500 to 1000 ms using an alpha Plan-Fluar 100x/1.45 Oil M27 (Zeiss, Oberkochen, Germany).

2.14 Differentiation, lipid staining, and quantification of iBACs

iBACs were cultured in growth medium (DMEM containing 25 mM glucose, 2 mM L-glutamine, 10% FBS, 50 μg/ml streptomycin, 50 units/ml penicillin, and 20 mM Hepes) at 37°C in 5% CO_2 atmosphere. Adipocyte differentiation was induced by culturing cells in growth medium supplemented with 0.5 mM 3-isobutyl-1-methylxanthine, 0.5 μM dexamethasone, 20 nM insulin, 1 nM triiodthyronine, and 125 μM indomethacin. After two days, cells were cultivated in growth medium supplemented with 20 nM insulin and 1 nM triiodothyronine until harvest. Full differentiation was achieved after 7 days. During the entire differentiation period cells were treated either with 30 μM Lalistat2 (10 mM stock in DMSO) or DMSO. Cells were incubated with 10 μM isoproterenol for 2 h to stimulate lipolysis. FFA and TG concentrations were determined using the NEFA-HR Kit (Wako Life Sciences, Mountain View, CA) and Infinity Triglyceride Reagent (Thermo Scientific, Waltham, MA), respectively. Values were normalized to total protein content (BCA reagent, Pierce, Rockford, IL). Lipid staining of fixed cells (10% formalin in PBS, 30 min) was performed using Oil red O (ORO; 0.25% in 60% isopropyl alcohol stock solution diluted 3:2 with dH2O) for 45 min.

2.15 Isolation, culture, and differentiation of stromal vascular cells

The isolation of adipose stromal vascular cells (SVCs) was performed as previously described [29] with some modifications. Subcutaneous WAT from female 8-10 week old mice was dissected, washed, minced, and digested in 1 ml PBS containing 0.125 U/ml collagenase D (Roche Diagnostics, Mannheim, Germany), 2.4 U/ml dispase II (Sigma-Aldrich, St. Louis, MO), and 10 mM $CaCl_2$ (Sigma-Aldrich, added just before tissue digestion) at 37°C under constant shaking at 180 rpm for 30 min. Digestion was stopped by the addition of complete DMEM/F12 containing Glutamax (LifeTechnology, Carlsbad, California), 10% FBS, and 1% penicillin/streptomycin. After centrifugation at 200 x *g* for 10 min, the pellet was resuspended in complete DMEM/F12, filtered through a 70-μm cell strainer, and centrifuged for 10 min at 700 x *g*. The cell pellet containing the SVCs was resuspended in complete DMEM/F12 and seeded on a 10-cm cell culture dish until a confluency of ~80%. SVCs were then seeded on 12-well plates until confluency. Differentiation was induced by incubating the SVCs with complete DMEM/F12 supplemented with 1 μM dexamethasone, 0.5 mM isobutylmethylxanthine (IBMX), 5 μg/ml insulin, and 1 μM rosiglitazone. Three days after induction, medium was changed to complete DMEM/F12 supplemented with 5 μg/ml insulin for two days. Afterwards, cells were maintained in complete DMEM/F12 until day 7, at which the fully differentiated SVCs were stained with ORO for neutral lipid visualization.

2.16 Statistics

Statistical analyses were performed using GraphPad Prism 5.0 software. Data are presented as mean ± SEM. Comparisons between 2 groups were performed using unpaired 2-tailed Student's t test. Paired Student's t test was used for comparisons of repeated measurements within the same group. Comparisons of multiple groups were analyzed by 2-way ANOVA followed by Bonferroni post-tests. Significance levels were set at $p < 0.05$ (*), $p \leq 0.01$ (**) and $p \leq 0.001$ (***).

3 Results

3.1 Transient drops in energy expenditure accompanied by hypothermic events in Lal-/- mice housed at RT

To investigate the effects of LAL deficiency on energy metabolism, we first housed WT and Lal-/- mice in metabolic cages at RT. In Lal-/- mice, we observed regular decreases in energy expenditure, which were most pronounced during fasting (Fig. 1A). Oxygen consumption followed the same pattern (Fig. S1). Respiratory exchange rate (RER) was also decreased in Lal-/- mice with more evident changes in the dark phase (Fig. 1B). As energy expenditure is positively correlated with BAT activity and thermogenesis, we measured core body temperature at different time points of the day. In accordance with reduced energy expenditure, we found decreased body temperature in Lal-/- mice at 9 a.m. (Fig. 1C). In addition, Lal-/- mice exhibited reduced locomotor activity during the dark phase (Fig. 1D) and comparable food intake (Fig. 1E). Lal-/- mice aged 20 weeks progressively loose WAT depots (Fig. 1F) [5, 10]. Fasting resulted in increased body weight loss in Lal-/- mice (Fig. 1G), suggesting that Lal-/- mice excessively utilize their adipose depots to maintain core body temperature upon fasting.

3.2 Intact BAT mass but altered brown adipocyte morphology in Lal-/- mice

It was previously reported that LAL deficiency in mice leads to progressive loss of BAT [5]. However, we found no difference in BAT mass between Lal-/- mice and controls (Fig. 2A) at the age of 20 weeks but numerous small LD in Lal-/- BAT (Fig. 2B). In accordance with our previous studies [10, 28], we found lipid-laden lysosomes in BAT of Lal-/- mice, distinguished from cytosolic LD by electron-dense phospholipid bilayers (Fig. 2B and S1B). Detailed size distribution analysis confirmed that predominantly small LDs are present in the BAT of Lal-/- mice (Fig. 2C) resulting in reduced total LD area (Fig. 2D).

To elucidate whether functional LAL is crucial for differentiation of brown adipocytes, we determined the *in vitro* effects of LAL inhibition on the differentiation capacity of iBACs using the LAL-specific inhibitor Lalistat2 [28, 30]. Intracellular neutral lipid content (Fig. S2A) and TG concentrations were comparable in Lalistat2-treated and control cells in the basal state and after β-adrenergic stimulation using isoproterenol (Fig. S2B). In the basal state, LAL inhibition resulted in decreased release of FA (Fig. S2C). LAL inhibition and Lalistat2 specificity in cells were confirmed by reduced acid (Fig. S2D) and unchanged neutral TG hydrolase activity (Fig. S2E) upon inhibitor treatment. Reduced WAT in Lal-/- mice may be a result of defective differentiation of precursor cells into white adipocytes. However, we found that Lal-/- and WT stromal vascular cells (SVCs) differentiated to similar extents (Fig. S2F), suggesting that reduced WAT mass in Lal-/- mice is independent of the differentiation capacity of precursor cells into white adipocytes. Moreover, *Lal* mRNA expression was unchanged during differentiation of WT SVCs (Fig. S2G). Together, these findings indicate that LAL is not required for brown and white adipocyte differentiation.

3.3 Markedly reduced UCP1 expression in BAT of Lal-/- mice housed at RT

The ability of BAT to sustain thermogenesis is dependent on UCP1 expression and activity [31]. Decreased core body temperature at RT (Fig. 1C) was associated with markedly reduced UCP1 protein expression in the BAT of Lal-/- mice (Fig. 2E). Since inflammation downregulates UCP1 expression [32, 33] and Lal-/- mice have a pro-inflammatory phenotype [34], we analyzed mRNA expression of inflammatory markers in BAT. As shown in Fig. 2F, we found increased expression of macrophage (*Emr1*) and inflammatory markers (*Il-1β*, *Tnf-α*) in BAT of Lal-/- mice already at the age of 7 weeks.

TG hydrolase activity at neutral pH was decreased by 66% in BAT of Lal-/- mice (Fig. 2G), suggesting low hydrolysis of LD-originating TG. Furthermore, in the fed state, Lal-/- mice had decreased plasma FFA (Fig. 2H), free glycerol (FG) (Fig. 2I), TG (Fig. 2J), and blood glucose (Fig. 2K) concentrations. These data suggest that decreased BAT thermogenesis and transient hypothermia in Lal-/- mice may be a consequence of markedly reduced UCP1 protein expression and activation as well as defective substrate mobilization.

3.4 Severe hypothermia in cold-exposed Lal-/- mice

We then housed the mice at 5°C (food and water *ad libitum*) and observed a striking drop in core body temperature in Lal-/- mice after only 4 h of cold exposure (Fig. 3A). Surprisingly, we found unchanged *Ucp1* mRNA expression, while analysis of genes involved in BAT activation revealed upregulation of *Crtc2*, *Pparγ* and its coactivator *Pgc1α* and a trend to

increased *Prdm16* gene expression in cold-exposed Lal-/- BAT (Fig. 3B). These results suggest that cold induces an increased signal towards activation of brown adipocytes in Lal-/- mice. As substrate availability is critical for maintaining optimal BAT function, we checked genes involved in autophagy, lysosomal activity, and LD hydrolysis. We found upregulated *Atg7* mRNA expression, indicating increased autophagy. Several markers such as the lysosomal master regulator *Tfeb*, *Lamp1*, *Lamp2*, *Mcoln1*, and the cytosolic lipases *Atgl* and *Hsl* were also upregulated in BAT of Lal-/- mice (Fig. 3C). In line with mRNA levels, UCP1 protein expression was comparable between the genotypes and LC3-II, a marker for autophagy, was substantially increased in Lal-/- mice (Fig. 3D). Elevated TG hydrolase activity at neutral pH indicates that BAT of cold-exposed Lal-/- mice strives to utilize lipid substrates to sustain thermoregulation (Fig. 3E). Plasma FFA concentrations as well as mRNA expression of the main FA transporters in BAT (*Fabp4*, *Cd36*) were comparable between both groups (Fig. 3F, G). Despite upregulation of the processes to generate lipid sources for heat production, Lal-/- mice cannot survive cold challenge, pointing out a crucial role for LAL in providing FA for BAT thermogenesis and UCP1 activation.

As the phenotype of Lal-/- mice worsens during aging, one might have expected young mice to be less cold intolerant than older mice. However, even 6 week old Lal-/- mice entered hypothermia after 3 h in the cold (Fig. S3A), confirming that thermogenesis is defective as a result of LAL deficiency in mice. We also analyzed BAT morphology in 6 week old mice housed at RT and found lipid-laden lysosomes and mitochondria with normal ultrastructure and cristae (Fig. S3B). We also observed slightly increased LD size and area (Fig. S3C, D). Thus, our data demonstrate that lysosomal lipid hydrolysis provides substrate for thermogenesis, irrespective of age and the cytosolic LD pool in BAT.

3.5 Lipid droplet depletion, decreased acetyl-CoA and increased acyl-carnitine concentrations in BAT of cold-exposed Lal-/- mice

Despite increased cellular mechanisms to provide energy substrates, cold exposure caused life-threatening hypothermia in Lal-/- mice. In sharp contrast to controls, electron micrographs from cold-exposed Lal-/- mice revealed reduced cytosolic LD and the presence of lipid-laden lysosomes in BAT (Fig. 4A). To better discriminate between LD and lysosomes, we performed immunofluorescence staining using perilipin 1 as LD marker and cathepsin D to track lysosomes. Increased cathepsin D staining revealed elevated number and size of lysosomes, whereas perilipin 1 staining indicated smaller LD in the BAT of Lal-/- mice. In particular, we observed ring-like structures positive for cathepsin D, indicative of lipid accumulation in lysosomes (Fig. 4B). Decreased acetyl-CoA concentration was in line with an energy deficit in BAT. We found altered concentrations of individual acyl-CoAs with increases in C16:0, C16:1, and C18:0 but reduced C18:2, whereas levels of total species were comparable between both genotypes (Fig. 4C). In contrast, concentrations of total acyl-carnitines were increased and various species were either unchanged or increased (Fig. 4D). To decipher if this was a result of accelerated FA binding to carnitine or an accumulation of carnitine esters due to impaired mitochondrial transport/processing, we analyzed the mRNA expression of several genes involved in these pathways. Increased mRNA expression of Cpt1b, which is responsible for transferring CoA-bound FA

Europe PMC Funders Author Manuscripts

to carnitine, indicates elevated trafficking of acyl-carnitines. mRNA expression levels of *Cpt2*, *Cact*, *Lcad*, and *Vlcad* (Fig. 4E) were unchanged in BAT of Lal-/- mice.

3.6 Decreased oxygen consumption and increased glucose uptake in BAT of cold-exposed Lal-/- mice

Besides lipids, glucose serves as important substrate for heat generation and cold exposure triggers glucose uptake in BAT [35]. We found markedly decreased blood glucose concentrations (Fig. 5A) in cold-exposed Lal-/- mice. We therefore hypothesized that glucose plays a crucial role in maintaining temperature homeostasis in Lal-/- mice. Indeed, both basal and FCCP-uncoupled oxygen consumption rates were decreased in a low-glucose (100 mg/ml) respiration medium compared to WT mice (Fig. 5B). An increased glucose concentration in the medium of 450 mg/ml normalized oxygen consumption in the BAT of Lal-/- mice (Fig. 5C), indicating that BAT from Lal-/- mice relies on glucose for respiration. To assess the effect of glucose supplementation *in vivo*, we injected mice i.p. with a single dose of glucose (2 g/kg body weight) prior to cold exposure, providing unlimited access to food. Lal-/- mice still entered hypothermia within 4 h of cold exposure (Fig. 5D), arguing that glucose slightly delays but does not compensate for the gap in energy demand of cold-exposed Lal-/- mice *in vivo.*

A prerequisite to improve cold tolerance of Lal-/- mice in the presence of glucose is an intact uptake of glucose into target organs such as BAT and skeletal muscle. We therefore performed glucose uptake studies in mice kept at 5°C. We observed increased radioactivity in BAT of Lal-/- mice and skeletal muscle (gastrocnemius) and inguinal WAT showed the same trend (Fig. 5E). In line with increased glucose incorporation into the BAT of Lal-/- mice, we found increased mRNA expression of *Glut-1* (Fig. 5F) and increased AKT phosphorylation (Fig. 5G). Our findings demonstrate that glucose supplementation cannot fully support thermogenesis when lipid catabolism in the lysosome is defective.

3.7 Altered muscle metabolism in cold-exposed Lal-/- mice

The trend to enhanced glucose uptake in skeletal muscle of cold-exposed Lal-/- mice pointed at increased metabolic activity. Thus, we analyzed acyl-CoAs and carnitine esters in skeletal muscle. We observed a major reduction of acetyl-CoA as well as of individual and total acyl-CoA concentrations (Fig. 5H), suggesting an intensified utilization of lipids to support shivering. Carnitine esters followed the opposite direction with an increase in all measured species (Fig. 5I). mRNA expression of genes involved in the regulation and processing of acyl-carnitines were unaltered, whereas the muscle proteolysis markers *Murf1* and *Atrogin1* were upregulated in Lal-/- mice (Fig. 5J). Creatine phosphokinase activity was markedly increased in the plasma of cold-exposed Lal-/- mice (Fig. 5K). These data indicate that during cold exposure Lal-/- mice utilize their muscle amino acids as additional source of energy and increase shivering to produce heat.

3.8 LAL deficiency aggravates dyslipidemia during cold exposure

BAT activation was reported to correct dyslipidemia in rodents [20, 22]. We therefore expected that cold might improve the observed hypercholesterolemia in Lal-/- mice. After cold exposure, however, plasma cholesterol and TG concentrations were increased (Fig. 6A),

whereas FG was decreased in Lal-/- mice (Fig. 6B), suggesting a defect in lipid clearance. Separation of lipoprotein species by fast protein liquid chromatography revealed disturbed lipoprotein distribution of both TC and TG with increased LDL and decreased HDL fractions in pooled plasma of Lal-/- mice (Fig. 6C, D). *Lpl* mRNA expression, however, was unchanged but angiopoietin-like 4 protein *(Angptl4)* transcript was 3.1-fold upregulated in BAT of Lal-/- mice (Fig. 6E). ANGPTL4 is highly expressed in BAT and is a powerful LPL inhibitor, thereby regulating circulating TG during cold exposure [36]. To visualize the fate of lipids, we gavaged cold-exposed mice with oil prior to organ collection. However, even after an oil gavage, BAT structure depicted the molecular observations, revealing impaired lipid uptake in BAT of Lal-/- mice (Fig. 6F). To precisely measure the extent to which lipid uptake is reduced in the BAT of cold-exposed Lal-/- mice, we gavaged the mice with [^{3}H]triolein and measured the FA incorporation into BAT. In accordance with the results from the micrographs, we found an 85% reduction in radioactivity in the BAT of Lal-/- mice compared to controls (Fig. 6G).

3.9 Decreased substrate oxidation and energy expenditure in Lal-/- mice during gradual cooling

Exposure to 5°C proved to be life threatening for Lal-/- mice and thus an additional stress by maintaining the mice in metabolic cages was impossible. We therefore decided to gradually decrease the ambient temperature over 7 days to 5°C. During the cooling period, Lal-/- mice visibly deteriorated and two of them died shortly after day 7. Indirect calorimetric measurements showed a decrease in RER and an obvious shift to the light phase, whereas WT mice preserved constant RER and circadian-regulated rhythm (Fig. 7A). Calculation of non-protein substrate oxidation using O_2 consumption and CO_2 release values revealed a clear defect in both carbohydrate and lipid oxidation (Fig. 7B, C). Furthermore, we observed reduced energy expenditure in both dark and light phases (Fig. 7D, E) and more than 40% reduction in locomotor activity (Fig. 7F) in Lal-/- mice. Body temperature measured at day 3 and 7 of the cooling period was decreased (Fig. 7G). Unlike WT mice, which gained weight during the experiment, Lal-/- mice lost on average 1.5 g of their body weight (Fig. 7H) and we found virtually no WAT depots in Lal-/- mice, despite comparable food intake between genotypes (Fig. 7I). These data suggest that LAL deficiency causes severe metabolic imbalance and ineffective substrate usage also during gradual temperature decrease.

4 Discussion

LAL hydrolyzes CE and TG within lysosomes to release FA and free cholesterol for catabolic, anabolic, and signaling purposes [37]. However, the role of LAL in the regulation of BAT-mediated thermogenesis is still underexplored. Lal-/- mice have been described to progressively lose WAT and BAT during aging [5]. Despite decreased WAT mass, our Lal-/- mice have intact interscapular and subscapular BAT depots, at least until 20 weeks of age, which provide a great opportunity to evaluate the contribution of LAL in overall thermogenesis. We observed regular drops in body temperature after the active phase in Lal-/- mice housed at RT. This finding might be explained (at least in part) by decreased energy expenditure and oxygen consumption.

The ability of BAT to maintain temperature homeostasis is insufficient both at RT and during cold exposure of Lal-/- mice, suggesting that alterations in lipid metabolism affect thermogenesis. Since neutral TG hydrolase activity is decreased in the BAT of Lal-/- mice, it is tempting to speculate that FA released by acid lipolysis in the basal state may serve as signaling molecules for neutral lipolysis. Beside β3 adrenergic stimulation, FA are important activators of UCP1-mediated heat generation in BAT [31]. Markedly decreased UCP1 expression at RT supports the hypothesis that hydrolysis products of LAL may play a role in the regulation of UCP1 expression/activity independent of the β3 adrenergic stimulatory cascade. Inflammation reduces UCP1 expression [32, 33] and LAL deficiency causes a severe inflammatory status in mice due to proliferation and infiltration of macrophages into various organs [34]. Despite increased macrophage and inflammation markers, UCP1 protein expression in BAT of cold-exposed Lal-/- mice was comparable to controls, suggesting that inflammation is not the sole factor driving UCP1 expression in Lal-/- mice. Comparable with our previous studies in macrophages and liver [10, 28] we observed increased number and size of lysosomes in BAT of Lal-/- mice. In contrast to controls, visualization of the lysosomal protease cathepsin D in BAT from Lal-/- mice revealed distinct ring-like structures, indicative of fatty lysosomes with entrapment of water-soluble proteins between lysosomal membrane and lipids.

Increased neutral TG hydrolase activity, reduced cytosolic LD, and accumulation of lipid-laden lysosomes in BAT because of LAL deficiency are associated with severe cold intolerance even in the presence of nutrients. In contrast, defective neutral lipolysis in AT-specific Atgl-/- mice resulted in cold intolerance only in the absence of food [38, 39], suggesting that exogenous nutrients are sufficient to refill BAT energy demands during cold exposure. Cold intolerance in young Lal-/- mice despite intact LD depots in BAT and only slightly reduced WAT mass argue against the assumption that decreased WAT depots are the main cause for cold-induced hypothermia in these mice. Reduced concentration of acetyl-CoA, an important fuel for mitochondrial respiration, might be caused by the observed hypoglycemia or ineffective FA oxidation and result in enhanced autophagy [40] in BAT of cold-exposed Lal-/- mice. Since autophagy promotes LD hydrolysis in AT [41], it is likely that a combined autophagy/lipolysis process increases the FA flux to mitochondria, as evidenced by elevated TG hydrolase activity and acyl-carnitine levels in BAT of Lal-/- mice.

In *ex vivo* studies, low glucose conditions (100 mg/dl) in the medium were insufficient for normal respiration in BAT from cold-exposed Lal-/- but not from WT mice, confirming that lipids are the preferred substrate for heat production in BAT. Interestingly, supra-physiological glucose concentrations (450 mg/dl) normalized respiration in BAT explants from Lal-/- mice. Cold exposure-mediated glucose uptake in BAT (via β3 adrenergic stimulation) is mainly executed by GLUT-1 [42]. Accordingly, mRNA expression of *Glut-1* and AKT phosphorylation were increased in BAT from Lal-/- mice, suggesting a compensatory upregulation of glucose metabolism. Despite increased glucose uptake into BAT *in vivo*, thermogenesis under cold exposure remained impaired, hinting toward a paramount role of LAL-derived FA in thermoregulation.

An increased uptake of glucose into skeletal muscle, reduced acyl-CoA concentrations together with elevated carnitine esters and proteolysis markers revealed an intense catabolic

activity in the skeletal muscle of Lal-/- mice. Activity of plasma creatine phosphokinase raised more than 2-fold compared to WT mice, implying pronounced shivering in Lal-/- mice. These findings suggest that under cold exposure, depletion of cytosolic LD in BAT and impaired substrate mitochondrial oxidation lead to defective thermogenesis, which cannot be compensated by incessant shivering as described for Ucp1-/- mice [43]. As we ruled out the possible interaction of Lalistat2 and neutral lipolysis *in vitro*, the reduced FA release in the basal state is highly attributed to LAL-dependent hydrolysis in iBACs. This provides evidence for the importance of LAL-derived FA with regard to energy supply and (most probably) signaling. Furthermore, given the detrimental effect of gradual cooling on whole-body metabolism in Lal-/- mice and defective substrate oxidation *in vivo*, we assume a central role for LAL in fuel recycling and compartmentalization in BAT specifically during cold exposure, independently of food intake.

Hypercholesterolemia is a well-documented feature of LAL-D patients [8] and normalizing plasma cholesterol concentrations would be essential as these patients are predisposed to early atherosclerosis [44]. Modulations of LAL activity in the arterial wall have been implicated in the progression of atherosclerotic lesions (reviewed in [45]). Since BAT activation had beneficial effects in mice models of atherosclerosis and dyslipidemia [20, 22], it was tempting to investigate whether a cold environment decreases circulating cholesterol levels in Lal-/- mice. Activated BAT enhances the selective uptake of FA from TRL, whereas the cholesterol-enriched remnant particles are cleared by the liver [19]. Cold exposure, however, aggravated dyslipidemia in Lal-/- mice, probably due to a defect in vascular lipolysis and/or clearance of lipoprotein remnants, as indicated by upregulated mRNA expression of *Angptl4* in BAT of Lal-/- mice. ANGPTL4 is a powerful LPL inhibitor and is highly expressed in BAT, where it is markedly suppressed by cold exposure, enhancing LPL activity and uptake of plasma TG-derived FA [36]. Consequently, we observed significantly increased plasma TG concentrations and reduced lipid uptake upon oil gavage in BAT of Lal-/- mice, suggesting a possible role of LAL as a regulator of *Angptl4* expression and, most probably, LPL activity. An interaction of ANGPTL4 with other lipases (e.g. ATGL, hepatic lipase, pancreatic lipase) has been previously postulated [46, 47]. It is currently unclear how the ANGPTL4-LPL-LAL axis may coordinate to channel FA into BAT to maintain thermogenesis. Future studies exploring the interaction between LAL and ANGPTL4 might open new molecular avenues as it is unknown whether *Angptl4* expression is affected in LAL-D patients. Their therapeutic options are rather limited to enzyme replacement therapy (ERT) as statin treatment brought little benefit in ameliorating dyslipidemia [44]. Since BAT activity in humans is positively correlated with metabolic health [48], it is plausible that defective BAT function additionally aggravates dyslipidemia in LAL-D patients. Our work helps understanding the critical features of LAL-D with respect to BAT dysfunction and related compensatory mechanisms developed by this condition. Whether ERT restores BAT function in mice (and/or humans) needs to be investigated in the future. Generation of tissue-specific Lal-/- mice will be of critical importance. These mice should help to elucidate tissue-specific effects, reveal whether circulating LAL compensates for its deficit in certain cells and organs, and determine whether variations in LAL activity contribute to the progression of atherosclerosis [45], non-alcoholic fatty liver disease, and non-alcoholic steatohepatitis [49].

In summary, global loss of LAL in mice leads to UCP1 downregulation and consequently decreased core body temperature at RT. Our data demonstrate that Lal-/- mice suffer from severe hypothermia within few hours of cold exposure, indicating that LAL is crucial for optimal BAT activity and its contribution to metabolic balance. We conclude that cold-dependent lipid clearance from the circulation depends on functional LAL.

Supplementary Material

Refer to Web version on PubMed Central for supplementary material.

Acknowledgements

This work was supported by the Austrian Science Fund FWF (DK-MCD W1226, P27070, P27108, P29328, I3165, SFB-LIPOTOX F30), the BioTechMed-Graz-funded flagship project “Lipases and Lipid Signaling”, and the PhD program “Molecular Medicine” of the Medical University of Graz. The authors thank Hong Du and Cong Yan (Indiana University School of Medicine, IN) for providing Lal-/- mice, Paul Helquist (University of Notre Dame, IN) for providing Lalistat2, and Patrick Seale (University of Pennsylvania, PA) for providing iBACs. The authors acknowledge the excellent technical assistance of S. Rainer, A. Ibovnik, Dominique Pernitsch, and Monika Siwetz (Medical University of Graz, Austria) and thank A. Absenger and I. Hindler (Medical University of Graz, Austria) for mice care.

References

[1]. Goldstein JL, Dana SE, Faust JR, Beaudet AL, Brown MS. Role of lysosomal acid lipase in the metabolism of plasma low density lipoprotein. Observations in cultured fibroblasts from a patient with cholesteryl ester storage disease. J Biol Chem. 1975; 250:8487–8495. [PubMed: 172501]

[2]. Brown MS, Goldstein JL. Receptor-mediated control of cholesterol metabolism. Science. 1976; 191:150–154. [PubMed: 174194]

[3]. Grumet L, Eichmann TO, Taschler U, Zierler KA, Leopold C, Moustafa T, Radovic B, Romauch M, Yan C, Du H, Haemmerle G, et al. Lysosomal Acid Lipase Hydrolyzes Retinyl Ester and Affects Retinoid Turnover. J Biol Chem. 2016; 291:17977–17987. [PubMed: 27354281]

[4]. Anderson RA, Rao N, Byrum RS, Rothschild CB, Bowden DW, Hayworth R, Pettenati M. In situ localization of the genetic locus encoding the lysosomal acid lipase/cholesteryl esterase (LIPA) deficient in Wolman disease to chromosome 10q23.2-q23.3. Genomics. 1993; 15:245–247. [PubMed: 8432549]

[5]. Du H, Heur M, Duanmu M, Grabowski GA, Hui DY, Witte DP, Mishra J. Lysosomal acid lipase-deficient mice: depletion of white and brown fat, severe hepatosplenomegaly, and shortened life span. J Lipid Res. 2001; 42:489–500. [PubMed: 11290820]

[6]. Du H, Duanmu M, Witte D, Grabowski GA. Targeted disruption of the mouse lysosomal acid lipase gene: long-term survival with massive cholesteryl ester and triglyceride storage. Hum Mol Genet. 1998; 7:1347–1354. [PubMed: 9700186]

[7]. Sloan HR, Fredrickson DS. Enzyme deficiency in cholesteryl ester storage idisease. J Clin Invest. 1972; 51:1923–1926. [PubMed: 5032533]

[8]. Bernstein DL, Hulkova H, Bialer MG, Desnick RJ. Cholesteryl ester storage disease: review of the findings in 135 reported patients with an underdiagnosed disease. J Hepatol. 2013; 58:1230–1243. [PubMed: 23485521]

[9]. Aguisanda F, Thorne N, Zheng W. Targeting Wolman Disease and Cholesteryl Ester Storage Disease: Disease Pathogenesis and Therapeutic Development. Curr Chem Genom Transl Med. 2017; 11:1–18. [PubMed: 28401034]

[10]. Radovic B, Vujic N, Leopold C, Schlager S, Goeritzer M, Patankar JV, Korbelius M, Kolb D, Reindl J, Wegscheider M, Tomin T, et al. Lysosomal acid lipase regulates VLDL synthesis and insulin sensitivity in mice. Diabetologia. 2016; 59:1743–1752. [PubMed: 27153842]

[11]. Cannon B, Nedergaard J. Brown adipose tissue: function and physiological significance. Physiol Rev. 2004; 84:277–359. [PubMed: 14715917]

[12]. Marzetti E, D'Angelo E, Savera G, Leeuwenburgh C, Calvani R. Integrated control of brown adipose tissue. Heart Metab. 2016; 69:9–14. [PubMed: 27524955]

[13]. Nedergaard J, Golozoubova V, Matthias A, Shabalina I, Ohba K, Ohlson K, Jacobsson A, Cannon B. Life without UCP1: mitochondrial, cellular and organismal characteristics of the UCP1-ablated mice. Biochem Soc Trans. 2001; 29:756–763. [PubMed: 11709070]

[14]. Shabalina IG, Backlund EC, Bar-Tana J, Cannon B, Nedergaard J. Within brown-fat cells, UCP1-mediated fatty acid-induced uncoupling is independent of fatty acid metabolism. Biochim Biophys Acta. 2008; 1777:642–650. [PubMed: 18489899]

[15]. Hoeke G, Kooijman S, Boon MR, Rensen PC, Berbee JF. Role of Brown Fat in Lipoprotein Metabolism and Atherosclerosis. Circ Res. 2016; 118:173–182. [PubMed: 26837747]

[16]. Christoffolete MA, Linardi CC, de Jesus L, Ebina KN, Carvalho SD, Ribeiro MO, Rabelo R, Curcio C, Martins L, Kimura ET, Bianco AC. Mice with targeted disruption of the Dio2 gene have cold-induced overexpression of the uncoupling protein 1 gene but fail to increase brown adipose tissue lipogenesis and adaptive thermogenesis. Diabetes. 2004; 53:577–584. [PubMed: 14988240]

[17]. Zimmermann R, Strauss JG, Haemmerle G, Schoiswohl G, Birner-Gruenberger R, Riederer M, Lass A, Neuberger G, Eisenhaber F, Hermetter A, Zechner R. Fat mobilization in adipose tissue is promoted by adipose triglyceride lipase. Science. 2004; 306:1383–1386. [PubMed: 15550674]

[18]. Nielsen TS, Jessen N, Jorgensen JO, Moller N, Lund S. Dissecting adipose tissue lipolysis: molecular regulation and implications for metabolic disease. J Mol Endocrinol. 2014; 52:R199–222. [PubMed: 24577718]

[19]. Scheja L, Heeren J. Metabolic interplay between white, beige, brown adipocytes and the liver. J Hepatol. 2016; 64:1176–1186. [PubMed: 26829204]

[20]. Bartelt A, Bruns OT, Reimer R, Hohenberg H, Ittrich H, Peldschus K, Kaul MG, Tromsdorf UI, Weller H, Waurisch C, Eychmuller A, et al. Brown adipose tissue activity controls triglyceride clearance. Nat Med. 2011; 17:200–205. [PubMed: 21258337]

[21]. Harms M, Seale P. Brown and beige fat: development, function and therapeutic potential. Nat Med. 2013; 19:1252–1263. [PubMed: 24100998]

[22]. Berbee JF, Boon MR, Khedoe PP, Bartelt A, Schlein C, Worthmann A, Kooijman S, Hoeke G, Mol IM, John C, Jung C, et al. Brown fat activation reduces hypercholesterolaemia and protects from atherosclerosis development. Nat Commun. 2015; 6:6356. [PubMed: 25754609]

[23]. Khedoe PP, Hoeke G, Kooijman S, Dijk W, Buijs JT, Kersten S, Havekes LM, Hiemstra PS, Berbee JF, Boon MR, Rensen PC. Brown adipose tissue takes up plasma triglycerides mostly after lipolysis. J Lipid Res. 2015; 56:51–59. [PubMed: 25351615]

[24]. Sachdev V, Leopold C, Bauer R, Patankar JV, Iqbal J, Obrowsky S, Boverhof R, Doktorova M, Scheicher B, Goeritzer M, Kolb D, et al. Novel role of a triglyceride-synthesizing enzyme: DGAT1 at the crossroad between triglyceride and cholesterol metabolism. Biochim Biophys Acta. 2016; 1861:1132–1141. [PubMed: 27344248]

[25]. Ferrannini E. The theoretical bases of indirect calorimetry: a review. Metabolism. 1988; 37:287–301. [PubMed: 3278194]

[26]. Prokesch A, Pelzmann HJ, Pessentheiner AR, Huber K, Madreiter-Sokolowski CT, Drougard A, Schittmayer M, Kolb D, Magnes C, Trausinger G, Graier WF, et al. N-acetylaspartate catabolism determines cytosolic acetyl-CoA levels and histone acetylation in brown adipocytes. Sci Rep. 2016; 6 23723.

[27]. Chandak PG, Radovic B, Aflaki E, Kolb D, Buchebner M, Frohlich E, Magnes C, Sinner F, Haemmerle G, Zechner R, Tabas I, et al. Efficient phagocytosis requires triacylglycerol hydrolysis by adipose triglyceride lipase. J Biol Chem. 2010; 285:20192–20201. [PubMed: 20424161]

[28]. Schlager S, Vujic N, Korbelius M, Duta-Mare M, Dorow J, Leopold C, Rainer S, Wegscheider M, Reicher H, Ceglarek U, Sattler W, et al. Lysosomal lipid hydrolysis provides substrates for lipid mediator synthesis in murine macrophages. Oncotarget. 2017; 8:40037–40051. [PubMed: 28402950]

[29]. Aune UL, Ruiz L, Kajimura S. Isolation and differentiation of stromal vascular cells to beige/brite cells. J Vis Exp. 2013

[30]. Rosenbaum AI, Cosner CC, Mariani CJ, Maxfield FR, Wiest O, Helquist P. Thiadiazole carbamates: potent inhibitors of lysosomal acid lipase and potential Niemann-Pick type C disease therapeutics. J Med Chem. 2010; 53:5281–5289. [PubMed: 20557099]

[31]. Nedergaard J, Golozoubova V, Matthias A, Asadi A, Jacobsson A, Cannon B. UCP1: the only protein able to mediate adaptive non-shivering thermogenesis and metabolic inefficiency. Biochim Biophys Acta. 2001; 1504:82–106. [PubMed: 11239487]

[32]. Nohr MK, Bobba N, Richelsen B, Lund S, Pedersen SB. Inflammation Downregulates UCP1 Expression in Brown Adipocytes Potentially via SIRT1 and DBC1 Interaction. Int J Mol Sci. 2017; 18

[33]. Sakamoto T, Takahashi N, Sawaragi Y, Naknukool S, Yu R, Goto T, Kawada T. Inflammation induced by RAW macrophages suppresses UCP1 mRNA induction via ERK activation in 10T1/2 adipocytes. Am J Physiol Cell Physiol. 2013; 304:C729–738. [PubMed: 23302779]

[34]. Yan C, Lian X, Li Y, Dai Y, White A, Qin Y, Li H, Hume DA, Du H. Macrophage-specific expression of human lysosomal acid lipase corrects inflammation and pathogenic phenotypes in lal-/- mice. Am J Pathol. 2006; 169:916–926. [PubMed: 16936266]

[35]. Stanford KI, Middelbeek RJ, Townsend KL, An D, Nygaard EB, Hitchcox KM, Markan KR, Nakano K, Hirshman MF, Tseng YH, Goodyear LJ. Brown adipose tissue regulates glucose homeostasis and insulin sensitivity. J Clin Invest. 2013; 123:215–223. [PubMed: 23221344]

[36]. Dijk W, Heine M, Vergnes L, Boon MR, Schaart G, Hesselink MK, Reue K, van Marken Lichtenbelt WD, Olivecrona G, Rensen PC, Heeren J, et al. ANGPTL4 mediates shuttling of lipid fuel to brown adipose tissue during sustained cold exposure. Elife. 2015; 4

[37]. Zechner R, Madeo F, Kratky D. Cytosolic lipolysis and lipophagy: two sides of the same coin. Nat Rev Mol Cell Biol. 2017

[38]. Ahmadian M, Abbott MJ, Tang T, Hudak CS, Kim Y, Bruss M, Hellerstein MK, Lee HY, Samuel VT, Shulman GI, Wang Y, et al. Desnutrin/ATGL is regulated by AMPK and is required for a brown adipose phenotype. Cell Metab. 2011; 13:739–748. [PubMed: 21641555]

[39]. Schreiber R, Diwoky C, Schoiswohl G, Feiler U, Wongsiriroj N, Abdellatif M, Kolb D, Hoeks J, Kershaw EE, Sedej S, Schrauwen P, et al. Cold-Induced Thermogenesis Depends on ATGL-Mediated Lipolysis in Cardiac Muscle, but Not Brown Adipose Tissue. Cell Metab. 2017; 26:753–763 e757. [PubMed: 28988821]

[40]. Marino G, Pietrocola F, Eisenberg T, Kong Y, Malik SA, Andryushkova A, Schroeder S, Pendl T, Harger A, Niso-Santano M, Zamzami N, et al. Regulation of autophagy by cytosolic acetyl-coenzyme A. Mol Cell. 2014; 53:710–725. [PubMed: 24560926]

[41]. Martinez-Lopez N, Garcia-Macia M, Sahu S, Athonvarangkul D, Liebling E, Merlo P, Cecconi F, Schwartz GJ, Singh R. Autophagy in the CNS and Periphery Coordinate Lipophagy and Lipolysis in the Brown Adipose Tissue and Liver. Cell Metab. 2016; 23:113–127. [PubMed: 26698918]

[42]. Dallner OS, Chernogubova E, Brolinson KA, Bengtsson T. Beta3-adrenergic receptors stimulate glucose uptake in brown adipocytes by two mechanisms independently of glucose transporter 4 translocation. Endocrinology. 2006; 147:5730–5739. [PubMed: 16959848]

[43]. Golozoubova V, Hohtola E, Matthias A, Jacobsson A, Cannon B, Nedergaard J. Only UCP1 can mediate adaptive nonshivering thermogenesis in the cold. FASEB J. 2001; 15:2048–2050. [PubMed: 11511509]

[44]. Valayannopoulos V, Malinova V, Honzik T, Balwani M, Breen C, Deegan PB, Enns GM, Jones SA, Kane JP, Stock EO, Tripuraneni R, et al. Sebelipase alfa over 52 weeks reduces serum transaminases, liver volume and improves serum lipids in patients with lysosomal acid lipase deficiency. J Hepatol. 2014; 61:1135–1142. [PubMed: 24993530]

[45]. Dubland JA, Francis GA. Lysosomal acid lipase: at the crossroads of normal and atherogenic cholesterol metabolism. Front Cell Dev Biol. 2015; 3:3. [PubMed: 25699256]

[46]. Kersten S. Regulation of lipid metabolism via angiopoietin-like proteins. Biochem Soc Trans. 2005; 33:1059–1062. [PubMed: 16246045]

[47]. Dijk W, Kersten S. Regulation of lipid metabolism by angiopoietin-like proteins. Curr Opin Lipidol. 2016; 27:249–256. [PubMed: 27023631]

[48]. Bartelt A, Heeren J. Adipose tissue browning and metabolic health. Nat Rev Endocrinol. 2014; 10:24–36. [PubMed: 24146030]

[49]. Baratta F, Pastori D, Del Ben M, Polimeni L, Labbadia G, Di Santo S, Piemonte F, Tozzi G, Violi F, Angelico F. Reduced Lysosomal Acid Lipase Activity in Adult Patients With Non-alcoholic Fatty Liver Disease. EBioMedicine. 2015; 2:750–754. [PubMed: 26288848]

Europe PMC Funders Author Manuscripts

Europe PMC Funders Author Manuscripts

Highlights

- Lal-/- mice have markedly reduced UCP1 expression when kept at room temperature
- Decreased lipid droplet size and accumulation of lysosomes in BAT of Lal-/- mice
- LAL deficiency causes BAT dysfunction and hypothermia in mice
- Functional LAL is required for cold-induced lipid clearance from circulation

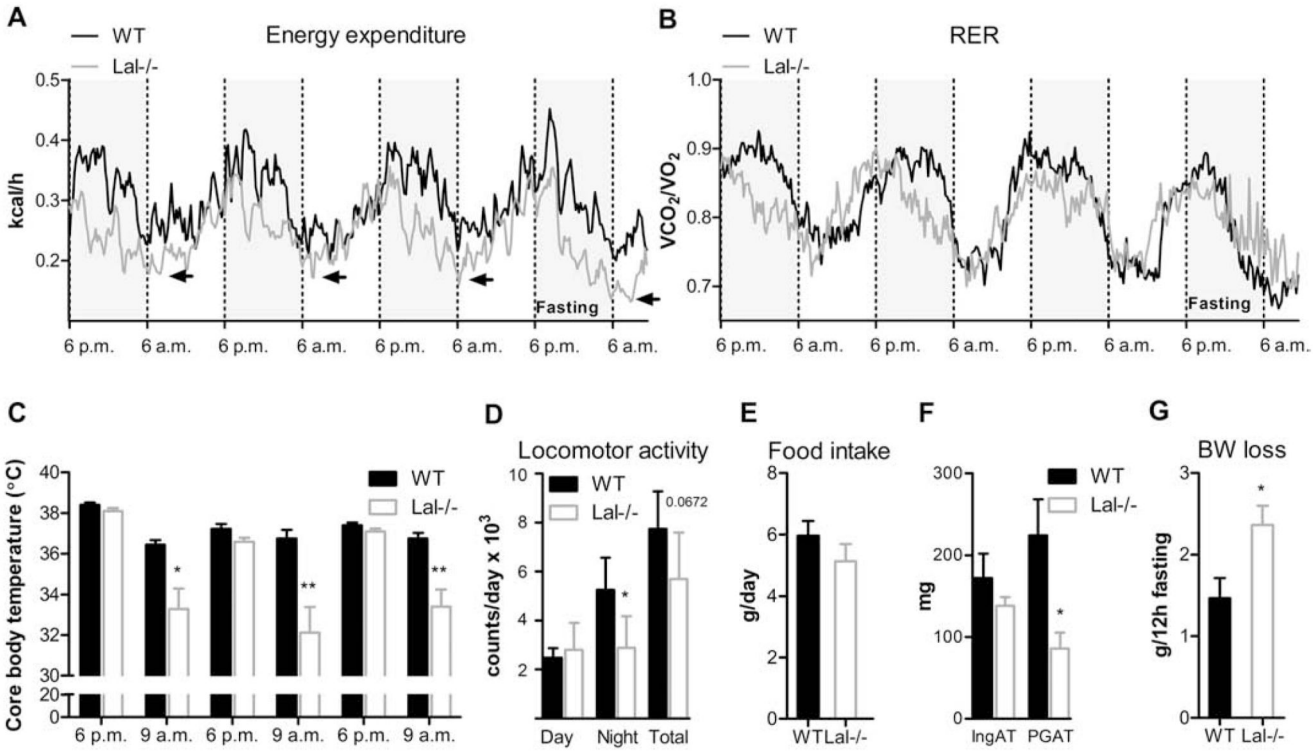

Figure 1. Decreased body temperature after the active phase in Lal-/- mice at room temperature.

Female WT and Lal-/- mice aged 20 weeks were housed at RT in metabolic cages with free access to chow diet. (**A**) Energy expenditure and (**B**) respiratory exchange rate (RER) measured by indirect gas calorimetry in WT (black line) and Lal-/- mice (grey line). Gray-shaded areas represent dark phase (6 p.m. - 6 a.m.); non-shaded, light phase (6 a.m. - 6 p.m.). Arrows represent transient drops in energy expenditure in Lal-/- mice. (**C**) Body temperature, (**D**) daily locomotor activity, and (**E**) food intake. (**F**) Weights of inguinal (ingAT) and perigonadal (PGAT) WAT (n=3). (**G**) Body weight loss after overnight fasting. Data represent mean + SEM (n=5-9); $p < 0.05$ (*), $p \leq 0.01$ (**). Student's unpaired t test.

Europe PMC Funders Author Manuscripts

Europe PMC Funders Author Manuscripts

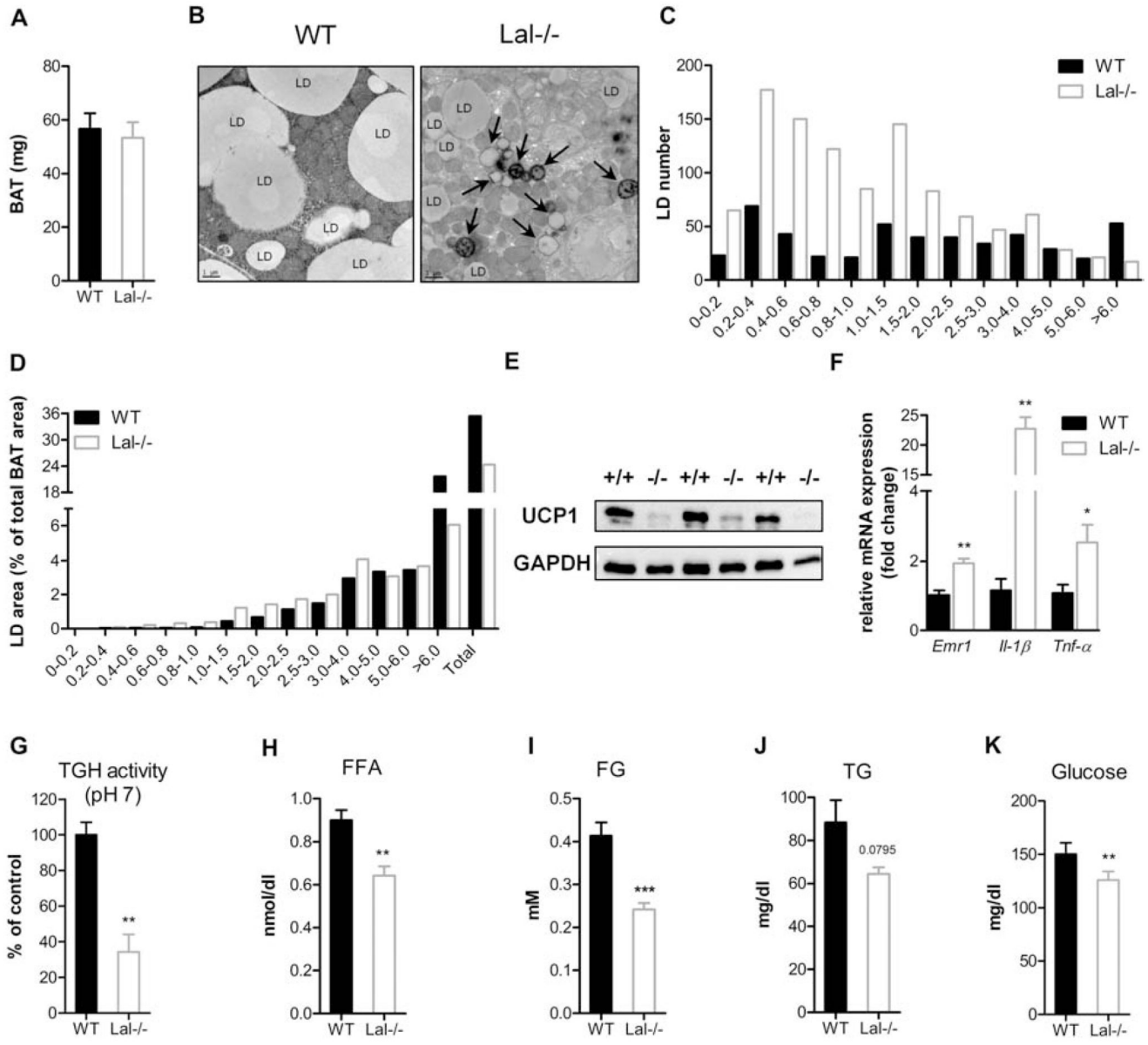

Figure 2. Lal-/- mice have altered BAT morphology and reduced UCP1 protein expression when kept at room temperature.

(**A**) BAT weight of 20 week old female mice (n=3). (**B**) Representative electron micrographs of BAT sections; scale bar, 1 μm; LD indicate cytosolic lipid droplets, arrows indicate lysosomes. (**C**) LD distribution and (**D**) LD surface in BAT calculated from 97 electron micrographs (each 142.09 μm^2) per genotype. (**E**) Immunoblotting against UCP1 using GAPDH as loading control. (**F**) mRNA expression of inflammatory markers in BAT of 7 week old male mice, relative to cyclophilin A expression as reference gene. Expression profiles were determined using the $2^{-\Delta\Delta Ct}$ method (n=3-4). (**G**) Neutral TG hydrolase activity in BAT (n=3) of 20 week old female mice. (**H**) Plasma free fatty acid, (**I**) free glycerol, (**J**) triacylglycerol, and (**K**) blood glucose concentrations were determined in the

fed state of 20 week old male mice (n=6). Data represent mean + SEM; $p < 0.05$ (*), $p \leq 0.01$ (**), $p \leq 0.001$ (***). Student's unpaired t test.

Europe PMC Funders Author Manuscripts

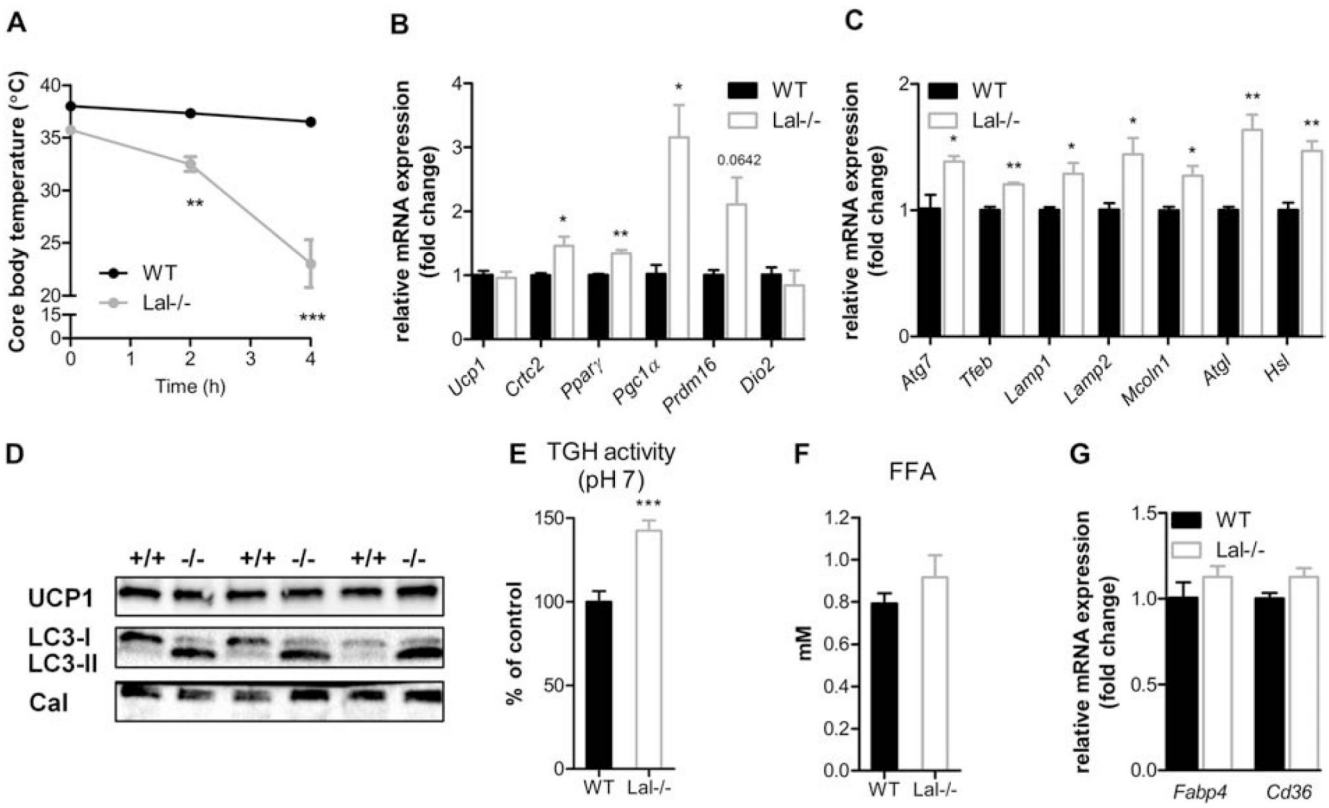

Figure 3. Lal-/- mice are cold intolerant despite comparable UCP1 expression and increased neutral lipolysis and autophagy in BAT.

Male WT and Lal-/- mice were acutely exposed to 5°C with free access to food and water. (**A**) Body temperature curves (n=6). After 4 h of cold exposure, mRNA expression of genes involved in (**B**) thermoregulation and (**C**) autophagy/lysosomal activity and neutral lipolysis in BAT, relative to cyclophilin A expression as reference gene. Expression profiles were determined using the $2^{-\Delta\Delta Ct}$ method (n=3). (**D**) Representative Western blots of UCP1, LC3-I, and LC3-II expression in BAT using calnexin as loading control. (**E**) Neutral TG hydrolase activity in BAT (n=5-7). (**F**) Plasma free fatty acid concentrations (n=6). (**G**) mRNA expression of genes involved in FA uptake. Data represent mean ± SEM; $p < 0.05$ (*), $p \leq 0.01$ (**), $p \leq 0.001$ (***). (A) ANOVA; (B, C, E, F, G) Student's unpaired t test.

Europe PMC Funders Author Manuscripts

Europe PMC Funders Author Manuscripts

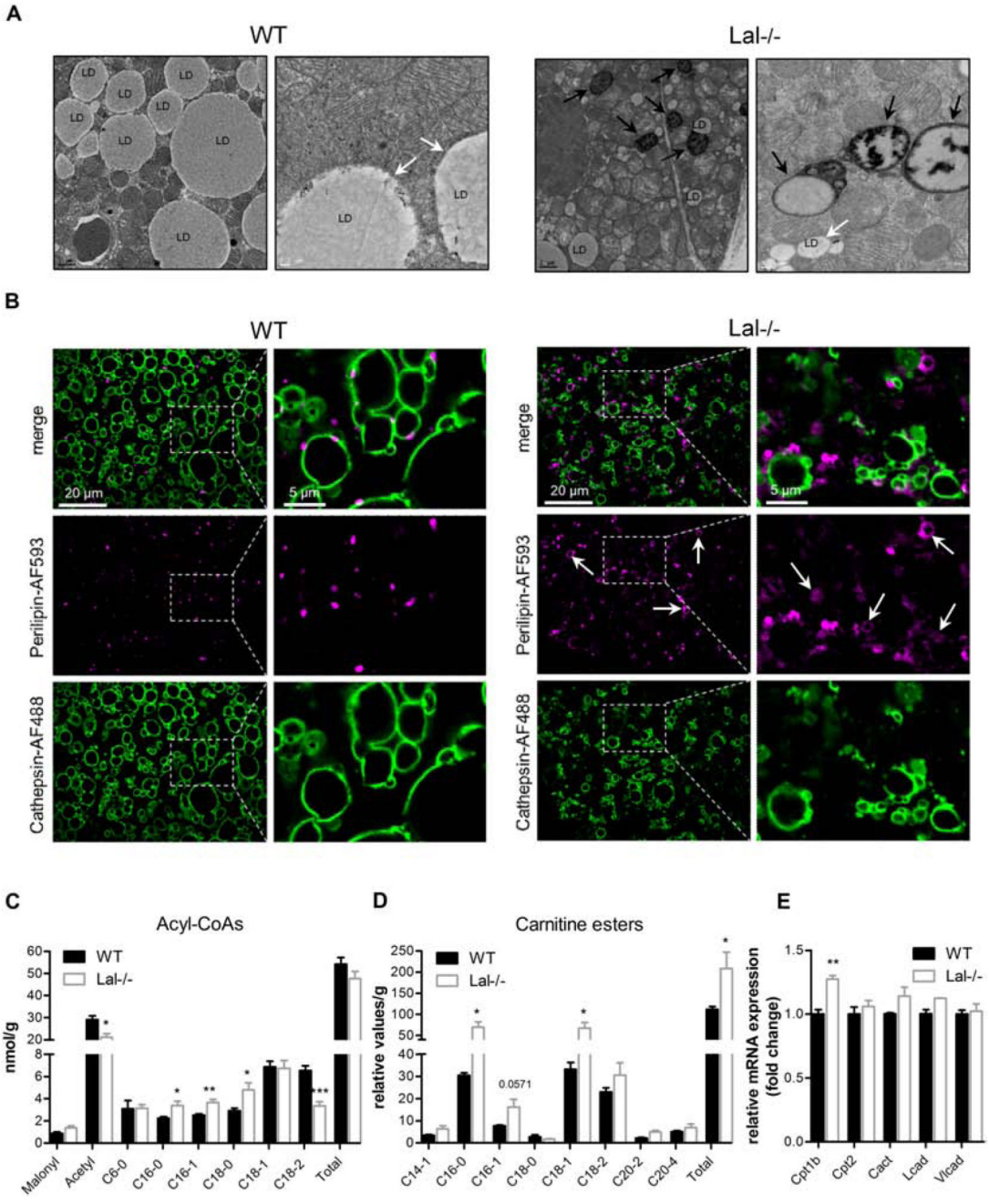

Figure 4. Cold exposure triggers lipid depletion and increases acyl-carnitines in the BAT of Lal-/- mice.

(**A**) Representative electron micrographs from BAT of mice exposed to cold for 4h. Scale bar, 1 μm; LD indicate cytosolic lipid droplets, white arrows indicate LD phospholipid monolayer, black arrows indicate electron-dense phospholipid bilayer of lysosomes. (**B**) Representative immunofluorescence micrographs of BAT using perilipin 1 as LD marker and cathepsin D as lysosomal marker. (**C**) Concentrations of acyl-CoAs and (**D**) carnitine esters (n=4-5). (**E**) mRNA expression of genes involved in FA mitochondrial trafficking and

oxidation, relative to cyclophilin A expression as reference gene. Expression profiles were determined using the $2^{-\Delta\Delta Ct}$ method (n=3). Data represent mean + SEM; $p < 0.05$ (*), $p \leq 0.01$ (**), $p \leq 0.001$ (***). Student's unpaired t test. B, E: male mice; A, C, D: female mice.

Europe PMC Funders Author Manuscripts

Europe PMC Funders Author Manuscripts

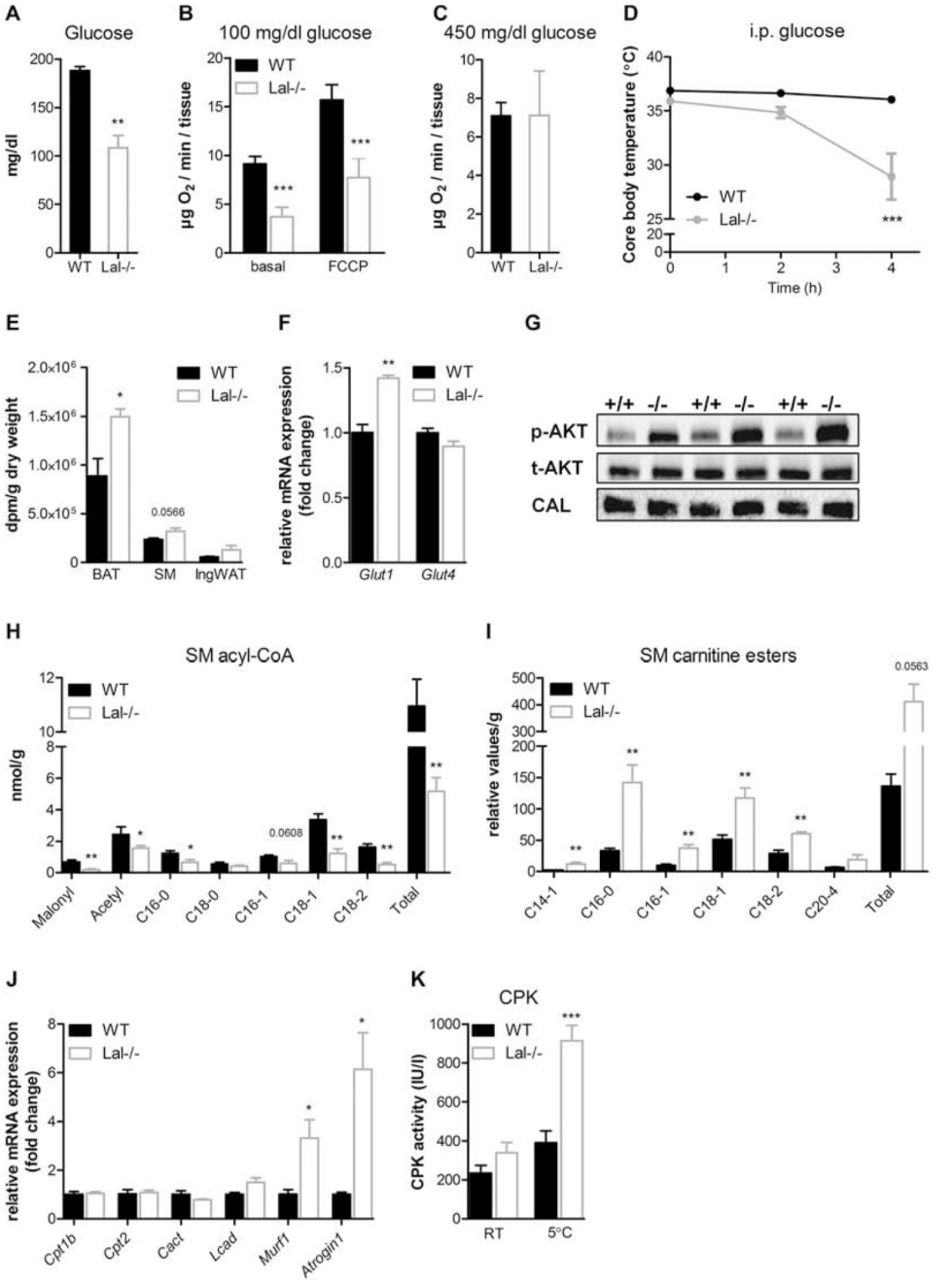

Figure 5. Cold exposure causes decreased BAT oxygen consumption but enhanced glucose uptake and compensatory shivering in Lal-/- mice.

WT and Lal-/- mice aged 20 weeks were exposed to cold for 4 h. (**A**) Blood glucose concentrations. BAT oxygen consumption in respiration buffer containing (**B**) 100 mg/dl or (**C**) 450 mg/dl glucose. (**D**) Core body temperature curves of mice injected i.p. with glucose (2 g/kg) and exposed to 5°C (n=5-6). (**E**) Radioactivity in BAT, gastrocnemius muscle (SM), and inguinal WAT (ingWAT) after i.p. injection of [^{3}H]2-deoxy-D-glucose (n=4). (**F**) mRNA expression of glucose transporters in BAT, relative to cyclophilin A expression as reference

gene. Expression profiles were determined using the $2^{-\Delta\Delta Ct}$ method (n=3). (**G**) Immunoblotting against phosphorylated (p) AKT and total (t) AKT in BAT using calnexin as loading control. (**H**) Acyl-CoA (n=5) and (**I**) carnitine ester (n-3-4) concentrations in skeletal muscle of WT and Lal-/- mice during cold exposure. (**J**) mRNA expression of genes involved in FA mitochondrial trafficking and oxidation and muscle proteolysis, relative to cyclophilin A expression as reference gene. Expression profiles were determined using the $2^{-\Delta\Delta Ct}$ method (n=3). (**K**) Plasma creatine phosphokinase (CPK) activity. Data represent mean ± SEM; $p < 0.05$ (*), $p \leq 0.01$ (**), $p \leq 0.001$ (***). (D) ANOVA, (A, B, C, E, F, H, I, J, K) Student's unpaired t test. A, C, F, G, J, K: male mice; B, D, E, H, I: female mice.

Europe PMC Funders Author Manuscripts

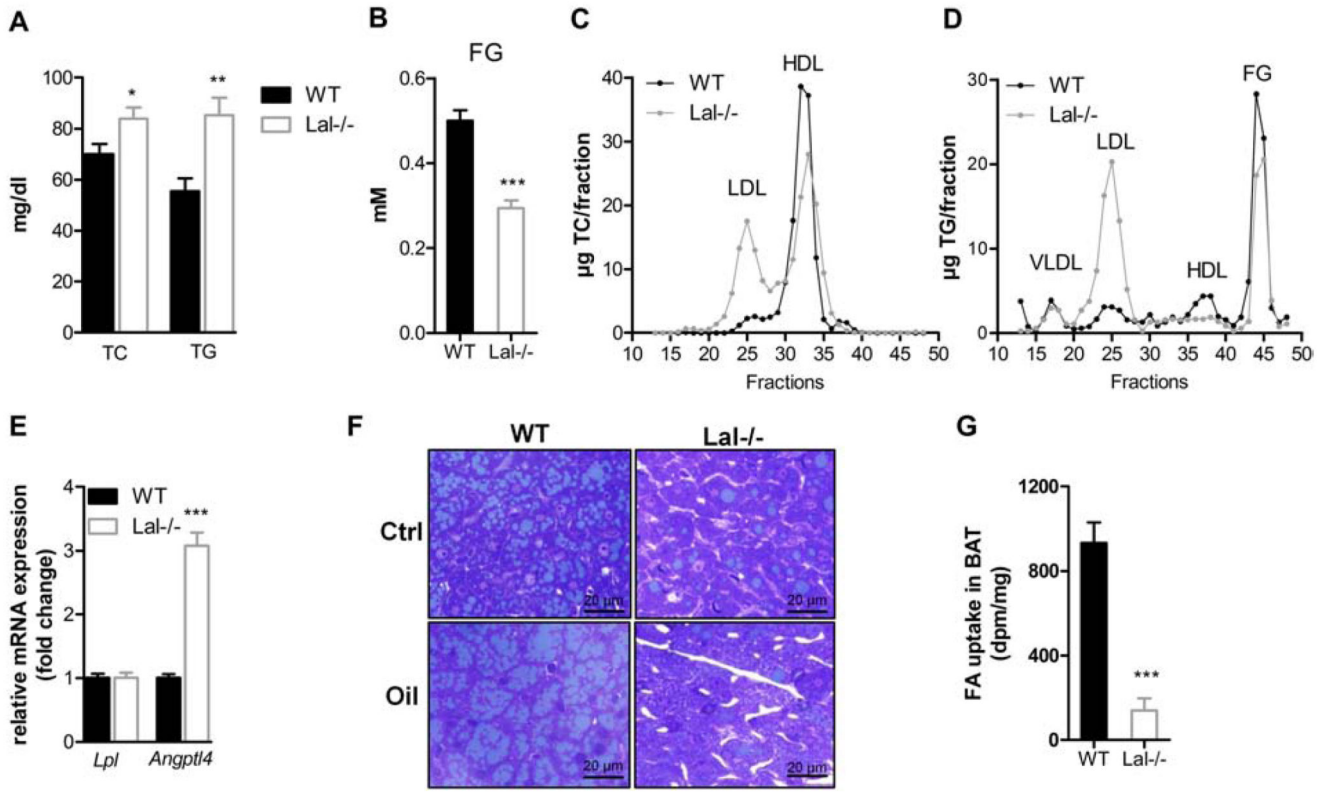

Figure 6. Cold exposure exacerbates dyslipidemia in Lal-/- mice due to impaired lipids uptake into BAT.

Male WT and Lal-/- mice were exposed to 5°C for 4 h. (**A**) Plasma cholesterol (TC), triacylglycerol (TG), and (**B**) free glycerol (FG) concentrations (n=6-8). Lipoprotein profiles of (**C**) TC and (**D**) TG after separation by fast performance liquid chromatography of pooled plasma (n = 6-7). (**E**) mRNA expression of lipoprotein lipase (*Lpl*) and angiopoietin-like 4 (*Angptl4*) in BAT, relative to cyclophilin A expression as reference gene. Expression profiles were determined using the $2^{-\Delta\Delta Ct}$ method (n=3). (**F**) Chow diet-fed WT and Lal-/- female mice were exposed to cold with or without an additional corn oil gavage (100 µl). Representative micrographs of toluidine bluestained BAT; magnification, 40x; scale bar, 20 µm. (**G**) FA uptake in BAT of cold-exposed female mice. Data represent mean + SEM; $p < 0.05$ (*), $p \leq 0.01$ (**), $p \leq 0.001$ (***). Student's unpaired t test.

Europe PMC Funders Author Manuscripts

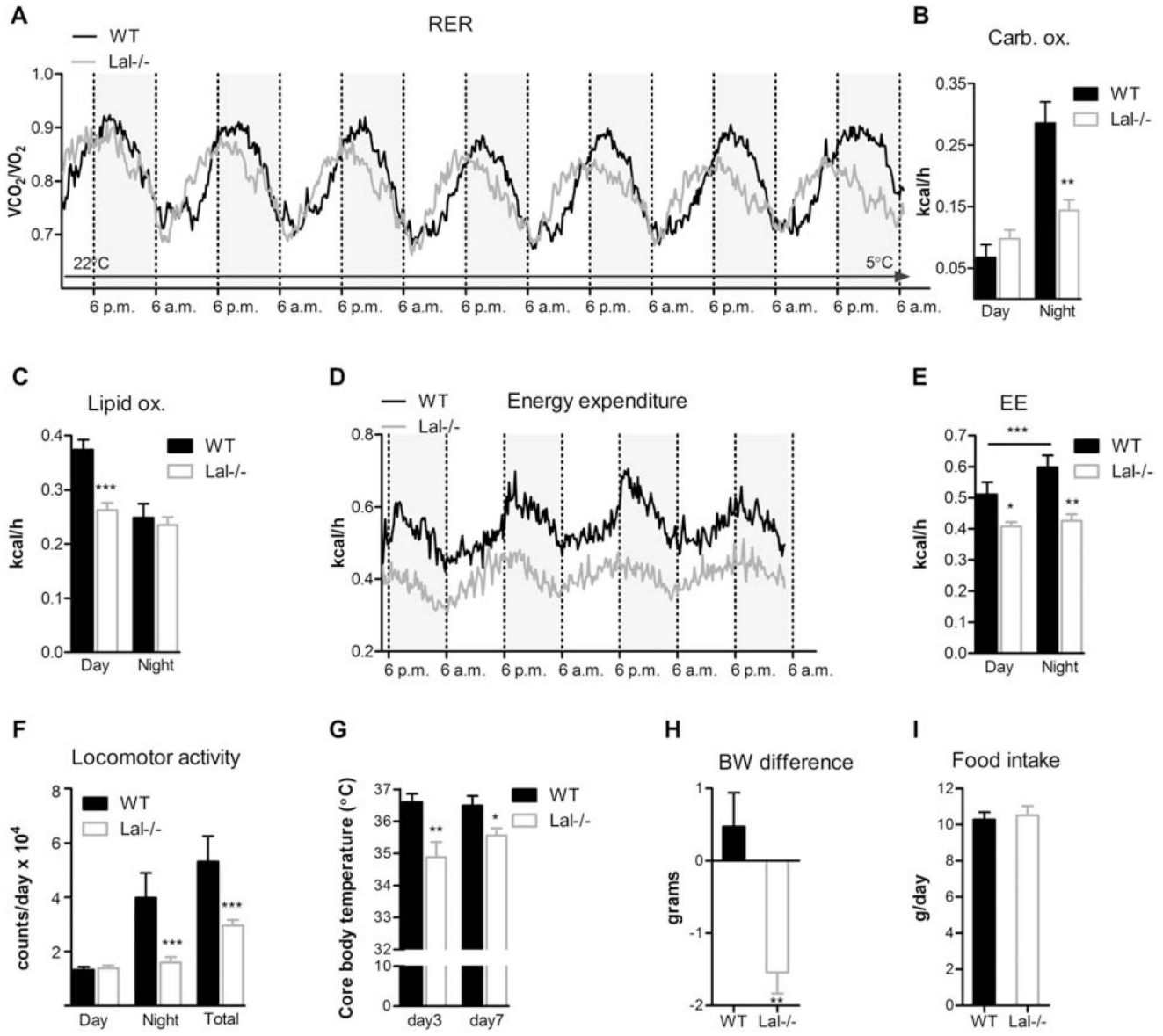

Figure 7. Gradual cooling causes decreased energy expenditure and core body temperature and increased weight loss in Lal-/- mice.

Female WT and Lal-/- mice were housed in metabolic cages and ambient temperature was gradually decreased from RT to 5°C over a period of 7 days. (**A**) Respiratory exchange rate (RER). Gray-shaded areas represent dark phase (6 p.m. - 6 a.m.); non-shaded, light phase (6 a.m. - 6 p.m.). Quantification of (**B**) carbohydrate and (**C**) lipid oxidation. Energy expenditure (**D**) curves and (**E**) average values. (**F**) Daily locomotor activity. (**G**) Body temperature measured during the cooling period. (**H**) Body weight difference and (**I**) daily food intake at the end of the cooling period (n=5-6). Data represent mean + SEM; $p < 0.05$ (*), $p \leq 0.01$ (**), $p \leq 0.001$ (***). Student's unpaired t test; (**E**) Repeated measurements for same genotype, Student's paired t test.